

# THEORETICAL EVALUATION OF THE INFLUENCE OF DISPLACEMENT ON FINGER PHOTOPLETHYSMOGRAPHY FOR WEARABLE HEALTH MONITORING SENSORS

Sokwoo Rhee, Boo-Ho Yang, and Haruhiko H. Asada

d'Arbeloff Laboratory for Information Systems and Technology  
Department of Mechanical Engineering  
Massachusetts Institute of Technology  
Cambridge, MA 02139, U.S.A.  
Email: sokwoo@mit.edu

## ABSTRACT

This paper describes the development of an opto-physiological model of a finger in conjunction with a ring-type photoplethysmography device (the Ring Sensor). This model is a combination of an optical model, a mechanical model, a skin capillary model and the arterial wall dynamics. It describes the photoplethysmographic effects due to the relative displacement and rotation of a finger to a ring-type opto-electric device that monitors the arterial pulsation noninvasively and continuously. Numerical simulations and experiments were conducted to verify and evaluate this model. This model can be used for optimizing design parameters of the ring device to obtain optimal pulse signals and to minimize the influence of noise caused by the displacement of the finger.

## INTRODUCTION

Finger photoplethysmography is a technique of noninvasively monitoring the arterial pulse of an individual that offers remarkable convenience and advantages. By integrating the technique with microelectronics and communication technologies, a miniaturized telemetered photoplethysmograph in a ring configuration has been developed by the authors [1] [2]. This device captures the pulsation of the arterial blood flow which is the AC part of photoplethysmography. The Ring Sensor, aiming at providing quality home healthcare, can be worn by the patient twenty-four hours a day. This is a unique form of wearable sensors and, probably, the only thing that the majority of people will accept wearing at all times. Real-time, continuous monitoring with the Ring Sensor allows not only for emergency detection but also for long-term monitoring of otherwise difficult and noncompliant patients such as demented elderly people. However, as a wearable ambulatory sensor, the Ring Sensor is inevitably subject to measurement noise due to the everyday activities of a patient. Especially, the relative displacement and the rotation of the sensor probe to the finger is the major cause of loss of accuracy, and a common problem for all other photoplethysmographic sensors such as pulse oximeters. The objective of the paper is to quantify the

mechanism of the motion artifact of finger photoplethysmography based on an opto-physiological model of the finger and to facilitate the development of the Ring Sensor which is less affected by the relative displacement of the finger to the ring.

There have been many attempts to analyze and reduce the influence of motion on the photoplethysmography. Many researchers attempted to quantify the movement artifact in pulse and oxygen saturation measurements [3][4], and some researchers have used advanced filtering techniques such as adaptive noise canceler to reduce the impact of motion [5]. However, those attempts did not help understand the nature of the motion artifact since they were based on the input-output matching approach using signal processing techniques without an in-depth understanding of the physiological effects of movement. Thus, it was not possible to conduct an optimization of the design parameters of the device for the best quality of measurement depending on those methods. In terms of modeling of photoplethysmography, Higgins, J. L. and Fronek, A. derived a mathematical formulation of reflectance photoplethysmography to evaluate the relationship between skin reflectance and skin blood flow [6]. However, their model was based on the modeling of cutaneous blood flow and does not account for the influence of arterial blood flow on the photoplethysmography.

In this paper, we first examine and categorize a variety of movements that influence photoplethysmographic signals of the Ring Sensor. To articulate and analyze the influence of each movement, we build a mathematical model of the finger photoplethysmography. The main feature of the model is the integration of multiple domains such as the ring mechanics, finger tissue kinematics, digital arterial wall dynamics and biomechanical optics. Especially, the nonlinear behavior of the arterial wall to external pressure, which is the basis of the oscillometric method of blood pressure measurement, is intensively addressed. Also, the optical property of the finger tissue is profoundly discussed. The resultant opto-physiological model of the finger and the Ring Sensor allows simulation of the influence of mechanical displacement of the finger on photoplethysmographic signals. Extensive simulation is conducted and the numerical results are



**Fig. 1: (a) Uncompressed finger under no external force ( $d=0$ ). (b) Finger compressed by the ring due to an external force ( $d>0$ )**

compared with the experimental data for the validation of the model at the end.

## APPROACH

One of the most important issues of wearable sensors is the reduction of noise caused by motion artifacts. Many kinds of motion artifacts such as fast and vivid motion of the finger, static relative displacement, and rotation of the ring relative to the finger can interfere with the measurement of the Ring Sensor. However, since the Ring Sensor is mainly to be worn by elderly patients and potential patients of cardiovascular disorders, it is reasonable to assume that the static displacement or rotation of the ring is dominant over fast movements with large accelerations. For example, if any external static force is applied to the ring so that the center point of the ring deviates from that of the finger, the photoplethysmographic signal will change. The rotation of the ring around the finger will also cause a change in the signal. A mathematical model of the finger and the ring will be very useful in understanding and analyzing the variation of the photoplethysmographic signal due to the displacement and the rotation of the ring. This model has to integrate all of the optical, mechanical and physiological properties of the Ring Sensor. In other words, the optics of the finger tissue and blood, finger tissue kinematics, geometry of the ring, and dynamics of the arteries and the capillaries must all be incorporated into one model to describe the photoplethysmographic behavior. Especially, the dynamics of the arterial wall should be modeled carefully since the compliance of the arterial wall exhibits nonlinear behavior [7]. The modeling of the optical properties is another point that has to be dealt with great care.

Fig. 1 shows a cross-sectional view of the finger. The cross section of a finger is assumed to be a circle when there are no external forces. There are two digital arteries in the finger, and they are both positioned at a distance  $h_0$  away from the center of the finger. The tissue is considered as compliant material with stiffness  $k_f$ . There is also a layer of capillaries of thickness  $t$  beneath the skin. To alleviate sensitivity of the photoplethysmographic signal variation due to movement of the finger, a compliant material of stiffness  $k_b$  is attached inside the solid ring. A light source (LED) and a photodetector are located on the compliant material inside the solid ring. When any external force is applied to the ring, it moves in a certain direction at an angle  $\alpha$  by a certain relative displacement  $d$ . Because of this movement, the pressure at contact point increases and the relative locations of the digital arteries to the optical elements (LED and

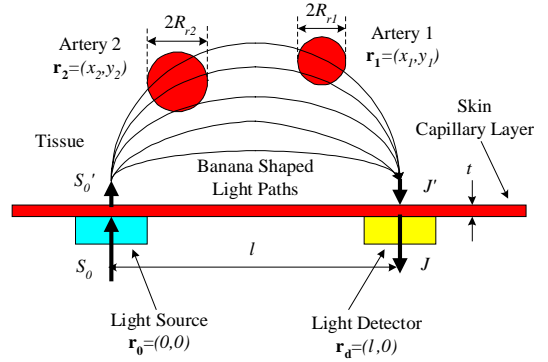


**Fig. 2: Optical model of the finger and optical elements. Blood vessels have different optical properties from the tissue**

photodetector) change, which leads to variation in the photoplethysmographic signal. At the same time, deformation of the finger surface occurs and the cross section of the finger is no longer a circle. Due to this deformation of the tissue, the pressure applied to each of the two digital arteries also changes, which results in a change in the volumetric pulsation of the blood vessel. In addition, the volume of capillaries also change due to the change of the pressure. The capillaries occlude more easily than digital arteries since the internal pressure of the capillary is much lower than that of the arteries. In this model, the occlusion of the capillaries is represented as the decrease of effective thickness of skin capillary layer  $t$ . The pulsating signal of photoplethysmograph is caused by the volumetric change of the digital arteries and capillaries due to the change of the blood pressure.

## MODELING

### Optical Model

The light emitted from the LED passes into the tissue and the number of the paths of photons is almost infinite, which makes it difficult to obtain a good optical model. The light absorption, multiple scattering, and diffusion processes all occur at the same time. It is known that the average photon migration path in the tissue is a banana shape. Assuming that the tissue is optically homogeneous, the cross section of a finger can be divided into three regions: tissue, two digital arteries, and capillaries. The blood that flows in the arteries has different optical properties from those of the tissue. Looking at the cross section of the finger, it is possible to consider the digital arteries as two circular regions with different optical properties from the surrounding material. Using the analogy with electrostatics, the photon flux density at the detector can be expressed as a function of the positions of the two arteries, radii of the arteries, the position of the photodetector, and the optical properties of the tissue and the blood. Feng, S., Zeng, F., and Chance, B. derived an analytical formulation of the photon path distributions in the presence of a spherical region with different absorption and scattering properties from the surroundings in semi-infinite geometry [8]. Fig. 2 shows the geometry of the light source, the photodetector, the arteries and the capillary layer. The light source is in the steady-state condition (constant source intensity of light  $S_0$ ) and is located at the origin  $\mathbf{r}_0=(0,0)$  of the x-y coordinate. The photon flux density at the detector which is located at  $\mathbf{r}_d=(l,0)$  is denoted as  $J$ . Although the LED and the photodetector are placed

along a circular ring surface, it is assumed that they are located on a straight line  $y=0$ . This assumption is valid as long as  $l$  is much smaller than the internal perimeter of the ring. As the light emitted from the source passes through the capillary layer of effective thickness  $t$  beneath the skin, the intensity decreases to  $S_0'$  due to the absorption by the blood in the capillaries. This absorption process follows the Lambert-Beer law. The scattering effect at the capillary layer is neglected since the thickness of the capillary layer is considerably thin ( $t \sim 0.1$  mm or less). The light of intensity  $S_0'$  which has passed through the capillary layer is injected and diffused into the tissue. The photons must pass through the capillary layer once again before it reaches the photodetector. The density of the photon flux entering the capillary layer is denoted as  $J'$  and it decreases by absorption process as the light goes through the capillary layer, resulting in a final photon flux density  $J$  at the detector.

In the analogy with electrostatics, the arteries are similar to the dielectric material in the electrical field. Noting the presence of two digital arteries which are located at  $\mathbf{r}_1=(x_1, y_1)$  and  $\mathbf{r}_2=(x_2, y_2)$  with radii of  $R_{r1}$  and  $R_{r2}$  respectively, the relationship between the light intensity  $S_0'$  (after passing through the capillary layer) and the photon flux density  $J'$  at the detector (before crossing the capillary layer) is described as follows.

$$J' = \frac{y_0 S_0'}{2\pi} \left\{ \frac{\kappa}{l^2} + \frac{1}{l^3} \int \exp(-\kappa l) + J_1(\mathbf{r}_1, R_{r1}) + J_1(\mathbf{r}_2, R_{r2}) \right\} \quad (1)$$

where the function  $J_1(\mathbf{r}, R)$  is as follows.

$$J_1(\mathbf{r}, R) = 2Dq(R) \frac{(\kappa|\mathbf{f}|+1)y}{|\mathbf{f}|^3} \exp(-\kappa|\mathbf{f}|) \Phi_0(\mathbf{r}) - 2Dp(R) \left\{ \frac{[\mathbf{f} \cdot \mathbf{E}_0(\mathbf{r})](\kappa|\mathbf{f}|+3)y}{|\mathbf{f}|^5} - \frac{E_0^y(\mathbf{r})}{|\mathbf{f}|^3} \right\} \exp(-\kappa|\mathbf{f}|) \quad (2)$$

where

$$\mathbf{r} = (x, y), \quad \mathbf{f} = \mathbf{r} - \mathbf{r}_d \quad (3)$$

$$\Phi_0(\mathbf{r}) = \frac{y_0 y S_0'}{2\pi D} \frac{(\kappa|\mathbf{r}|+1)}{|\mathbf{r}|^3} \exp(-\kappa|\mathbf{r}|) \quad (4)$$

where  $y_0 = 0.7 / \mu_s'$ ,

$$\mathbf{E}_0(\mathbf{r}) = (E_0^x, E_0^y) = \frac{y_0 S_0'}{2\pi D} \left\{ \frac{3\kappa y \mathbf{r}}{|\mathbf{r}|^4} + \frac{3y \mathbf{r}}{|\mathbf{r}|^5} - \frac{\kappa \hat{y}}{|\mathbf{r}|^2} - \frac{\hat{y}}{|\mathbf{r}|^3} + \frac{\kappa^2 y \mathbf{r}}{|\mathbf{r}|^3} \right\} \exp(-\kappa|\mathbf{r}|) \quad (5)$$

$$q(R) = -R \exp(\kappa R) \left\{ \frac{\tilde{D}B(1 - \mu_a / \tilde{\mu}_a)}{D(1 + \kappa R) \sinh(\tilde{\kappa}R) / (\tilde{\kappa}R) + \tilde{D}B} \right\} \quad (6)$$

$$p(R) = R^3 \exp(\kappa R) \left\{ \frac{\tilde{D}A - DB}{\tilde{D}A(1 + \kappa R) + DB[2 + 2\kappa R + (\kappa R)^2]} \right\} \quad (7)$$

where the coefficients A and B are given respectively,

$$A = \frac{2 \sinh(\tilde{\kappa}R)}{(\tilde{\kappa}R)} + \tilde{\kappa}R \sinh(\tilde{\kappa}R) - 2 \cosh(\tilde{\kappa}R) \quad (8)$$

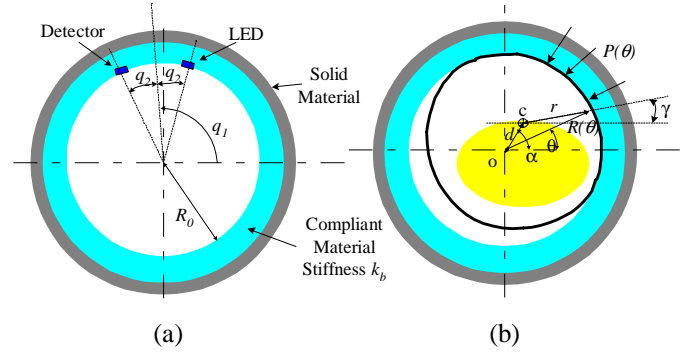


**Fig. 3 : (a) Initial state of the ring with LED and photodetector (b) When the finger moves in the ring (Finger tissue is deformed.)**

$$B = \cosh(\tilde{\kappa}R) - \frac{\sinh(\tilde{\kappa}R)}{(\tilde{\kappa}R)} \quad (9)$$

$\mu_a$  : Absorption coefficient of tissue

$\mu_s'$  : Transport scattering coefficient of tissue

$\tilde{\mu}_a$  : Absorption coefficient of blood

$\tilde{\mu}_s'$  : Transport scattering coefficient of blood

$D$  : Diffusion constant of tissue ( $= 1/[3(\mu_a + \mu_s')]$ )

$\tilde{D}$  : Diffusion constant of blood ( $= 1/[3(\tilde{\mu}_a + \tilde{\mu}_s')]$ )

$\kappa$  : Inverse diffusive absorption distance of tissue ( $= (\mu_a / D)^{1/2}$ )

$\tilde{\kappa}$  : Inverse diffusive absorption distance of blood ( $= (\tilde{\mu}_a / \tilde{D})^{1/2}$ )

Detailed derivations of Eqs. (1)~(9) can be found in [8].

The absorption process of the capillary layer defines the relationship between  $S_0$  and  $S_0'$ .

$$S_0' = S_0 \exp(-\tilde{\mu}_a t) \quad (10)$$

The final photon flux density is also obtained by the similar equation.

$$J = J' \exp(-\tilde{\mu}_a t) \quad (11)$$

As the absorption coefficient of blood is larger than that of tissue, the DC value of  $J$  increases as the two arteries are located farther from the origin, since more photons reach the detector without passing through the digital arteries. It is also natural that  $J$  increases as the radii of the arteries decrease. However, the amplitude of the AC component of  $J$  decreases as the distance of the arteries from the origin increases, since the change of the diameters of the arteries (which eventually results in the change of the extent of photon absorption) at distant locations does not give significant influence on the photons that reach the detector.

### Tissue Mechanical Model

The initial shape of the ring is shown in Fig. 3(a). The LED and the detector are placed such that their mid-point is at an angle  $q_1$  (rad) from the horizontal axis, and both the LED and the detector are at an

angle  $q_2$  (rad) from the radial line that intersects the mid point. As the finger moves inside the ring, the pressure at the contact point increases and both the finger tissue and the compliant material inside the ring go through deformation. This is shown in Fig. 3(b).

$O$  is the center of the ring and  $c$  is the reference point (initial center pint) of the finger located at the bone. As the reference point of finger moves by displacement  $d$  at an angle  $\alpha$ , the distance  $r$  (represented as a function of  $\gamma$ ) from the reference point of the finger to the skin changes from its initial value  $r_0$ . At the same time, the compliant material inside the ring also deforms and the distance  $R$  (represented as a function of  $\theta$ ) from the center of the ring to the ring inner material also deviates from its initial value  $R_0$ . Denoting the pressure at the contact as  $P$ , we can get the force equilibrium equation,

$$\begin{aligned} P &= [r_0 - r]k_t = [R - R_0]k_b \\ P &\geq 0, \text{ always } (r \leq r_0 \text{ and } R \geq R_0, \text{ always}) \\ P(\gamma) &= [r_0 - r(\gamma)]k_t : P \text{ as a function of } \gamma \\ P(\theta) &= [R(\theta) - R_0]k_b : P \text{ as a function of } \theta \end{aligned} \quad (12)$$

where  $k_t$  is the stiffness of the finger tissue and  $k_b$  is the stiffness of the compliant material inside the ring. From Eq. (12), we can get the following relationship.

$$R = R_0 + (r_0 - r) \left\{ \frac{k_t}{k_b} \right\} \quad (13)$$

From the kinematics of the tissue, we can also get the following equations.

$$r^2 = R^2 + d^2 - 2Rd \cos(\alpha - \theta) \quad (14)$$

$$R^2 = r^2 + d^2 - 2rd \cos(\pi - (\alpha - \gamma)) \quad (15)$$

Combining Eqs. (13), (14), and (15), the information about the deformation of the finger tissue and the ring inner material is obtained.

$$R(\theta) = \frac{(r_0 + R_0)^2 - d^2}{2[R_0 + r_0 - d \cos(\alpha - \theta)]} \quad \text{if } k_b = k_t \quad (16a)$$

$$R(\theta) = \frac{b - \sqrt{b^2 - ac}}{a} \quad \text{if } k_b \neq k_t \quad (16b)$$

where,

$$a = \left\{ \frac{k_b}{k_t} \right\}^2 - 1,$$

$$b = R_0 \left\{ \frac{k_b}{k_t} \right\}^2 + r_0 \left\{ \frac{k_b}{k_t} \right\} - d \cos(\alpha - \theta),$$

$$c = r_0^2 + R_0^2 \left\{ \frac{k_b}{k_t} \right\}^2 + 2R_0 r_0 \left\{ \frac{k_b}{k_t} \right\} - d^2$$

and,

$$r(\gamma) = \frac{(r_0 + R_0)^2 - d^2}{2[R_0 + r_0 + d \cos(\alpha - \gamma)]} \quad \text{if } k_b = k_t \quad (17a)$$

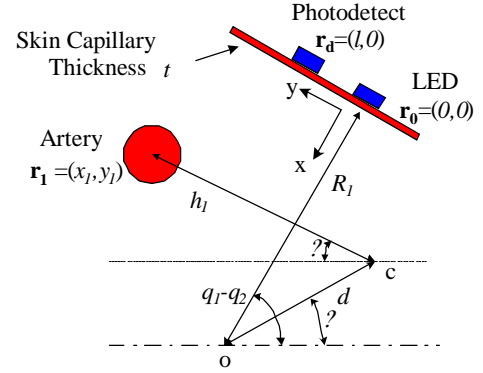


**Fig. 4 : Geometry of the LED, the photodetector, the artery 1, and the skin capillary layer**

$$r(\gamma) = \frac{b' - \sqrt{b'^2 - a'c'}}{a'} \quad \text{if } k_b \neq k_t \quad (17b)$$

where,

$$a' = \left\{ \frac{k_t}{k_b} \right\}^2 - 1,$$

$$b' = R_0 \left\{ \frac{k_t}{k_b} \right\}^2 + r_0 \left\{ \frac{k_t}{k_b} \right\} + d \cos(\alpha - \gamma),$$

$$c' = R_0^2 + r_0^2 \left\{ \frac{k_t}{k_b} \right\}^2 + 2R_0 r_0 \left\{ \frac{k_t}{k_b} \right\} - d^2$$

As shown in Fig. 4, the location of the artery 1 which is  $\mathbf{r}_1 = (x_1, y_1)$  in the optical model given by Eq. (1), can be derived using simple kinematics.

$$x_1 = d \sin[\alpha - (q_1 - q_2)] + h_1 \sin[\beta + (q_1 - q_2)] \quad (18a)$$

$$y_1 = R_1 - d \cos[\alpha - (q_1 - q_2)] + h_1 \cos[\beta + (q_1 - q_2)] \quad (18b)$$

where,

$$R_1 = R(q_1 - q_2) \text{ from Eqs. (16a) and (16b)}$$

$$h_1 = h_0 \left\{ \frac{r_1}{r_0} \right\}$$

where,

$$r_1 = r(\pi - \beta), \text{ from Eqs. (17a) and (17b)}$$

The location of the artery 2 which is  $\mathbf{r}_2 = (x_2, y_2)$  can also be obtained using similar derivations.

### **Dynamics of the Arterial Wall and the Capillary Layer**

The compliance of the arterial wall changes nonlinearly. There are many factors that influence the arterial wall compliance [9], such as temperature, pressure, or even emotion of the person. Among them, pressure is one of the most sensitive factors that change the compliance dramatically. Depending on the transmural pressure  $P_t$ , which is defined as the difference between the internal pressure  $P_i$  and

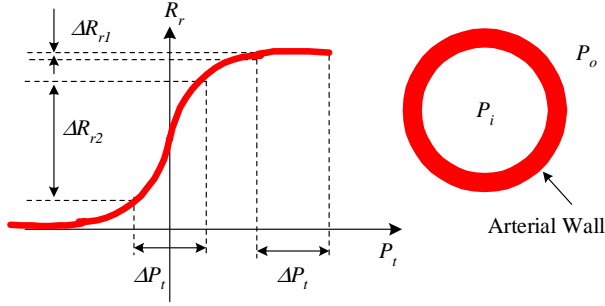


**Fig. 5 : Change of arterial wall radius ( $R_r$ ) with transmural pressure ( $P_t$ )**

external pressure  $P_o$ , the diameter changes of the digital artery differ even with the same change in blood pressure. Fig. 5 shows the relationship between the arterial wall radius  $R_r$  and the transmural pressure  $P_t$  [7][10]. As shown in the figure, even with the same change of transmural pressure  $\Delta P_t$ , the change of the arterial radii,  $\Delta R_{r1}$  and  $\Delta R_{r2}$ , are different depending on the operating point of  $P_t$ . The maximum arterial pulsation occurs approximately when the transmural pressure is zero. After this point, the arterial pulsation begins to diminish since the artery becomes occluded by the excessive external pressure [7][10]. This is a well-known principle used in oscillometric blood pressure measurement devices.

The internal pressure of the artery, which is actually what we define as “blood pressure”, is not actively controllable. However, we can change the amplitude of the volumetric pulsation of the artery by changing the external pressure  $P_o$  even under the same blood pressure. In our ring configuration, as the displacement  $d$  increases, the pressure around the contact point increases. This also changes the pressure applied to the digital arteries depending on the configuration and position of the ring. To calculate the radii of the arteries ( $R_{r1}$  and  $R_{r2}$  in Eq. (1)),  $P(\gamma)$  when  $\gamma=\pi-\beta$  and  $\gamma=\beta$  must be calculated from Eq. (12), and this becomes the external pressure  $P_{o1}$  and  $P_{o2}$  applied to digital artery 1 and 2 respectively.

In this approach, we model the relationship of  $R_r$  and  $P_t$  as a sigmoid function for simplicity.

$$R_r = \frac{C_1}{1 + \exp(-C_2(P_t - C_3))} \quad (19)$$

where

$$P_t = P_i - P_o$$

$P_i$  : blood pressure inside artery  
 $P_o$  : pressure outside of artery  
 $R_r$  : radius of digital artery

Finally,  $R_{r1}$  and  $R_{r2}$  in Eq. (1) can be described as follows.

$$R_{r1} = R_r(P_i - P_{o1}) \quad (20a)$$

$$R_{r2} = R_r(P_i - P_{o2}) \quad (20b)$$

where,

$$P_{o1} = (r_0 - r_1)k_t, \quad P_{o2} = (r_0 - r_2)k_t, \text{ from Eq. (12)}$$

where,

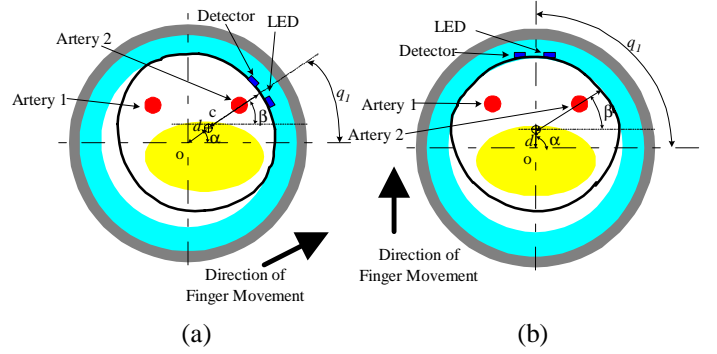


**Fig. 6 : Two cases of finger movements in the ring**  
**(a) Case 1 :  $\alpha = \beta = q_1$ ,  $q_2 = 10^\circ$**   
**(b) Case 2 :  $\alpha = q_1 = 90^\circ$ ,  $q_2 = 10^\circ$**

$$r_1 = r(\pi - \beta), \quad r_2 = r(\beta), \text{ from Eqs. (17a) and (17b)}$$

The effective thickness  $t$  of the capillary layer can also be obtained using similar derivations except that the operating range of the  $P_i$  is different from that of digital artery. The internal pressure  $P_i$  in digital artery oscillates in the range of 80~120 mmHg. However,  $P_i$  of the capillaries is around 10~35 mmHg, which makes the capillaries occlude more easily in the presence of an external pressure.

Combining the mechanical model describing the locations of the two arteries, the arterial wall dynamics equations given by Eqs. (20a) and (20b), and the optical model equations given by Eqs. (1), (10), and (11), the whole model is completed.

## NUMERICAL SIMULATION AND VERIFICATION BY EXPERIMENT

Numerical simulations and experiments were conducted with different angles of movements. The numerical simulations were performed using MATLAB version 5.2. The first case (Fig. 6a) is when the direction of movement is aligned with that of a digital artery. In the second case (Fig. 6b), the finger moves in the direction of the mid-point of two digital arteries. In the numerical simulations, the blood pressure (internal pressure  $P_i$ ) is given as a combination of two sinusoidal functions, one with a frequency of 1.2 Hz and the other 2.4 Hz. By this combination, we can closely simulate the two-peak feature of a real heart beat. For the optical coefficients, realistic values of  $\mu_a = 0.01/mm$ ,  $\mu_s = 0.7/mm$ ,  $\tilde{\mu}_a = 1.2/mm$ , and  $\tilde{\mu}_s = 1.2/mm$  are used in the numerical simulations. In the experiments, the LED and the photodetector are closely packed in a sensor unit board, and the ring is positioned so that the sensor is aligned in the direction of movement in each case. ( $\alpha=q_1$ )

### Analysis of the Simulation and Experiment : Case 1

When the direction of finger movement is aligned with the location of a digital artery ( $\alpha=\beta$ ), it is expected that the amplitude of the photoplethysmograph will change greatly as  $d$  (displacement) increases due to two reasons. First, as the sensor is aligned with a digital artery, the distance from the artery and the photodetector will decrease significantly as  $d$  increases. This will result in a more change of light absorption by the blood with the same change of the diameter

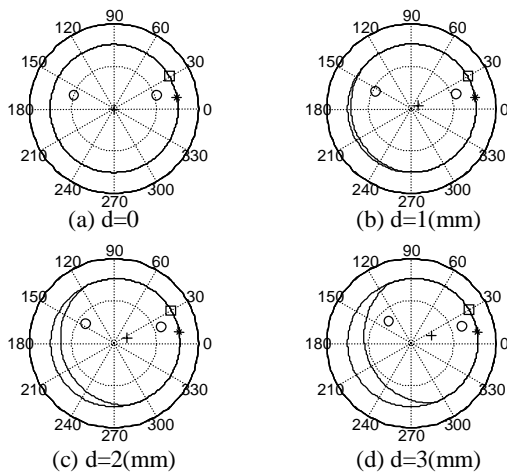


**Fig. 7 : Visualization of movement at case 1. It is shown that the finger shape becomes more oval as  $d$  increases.**

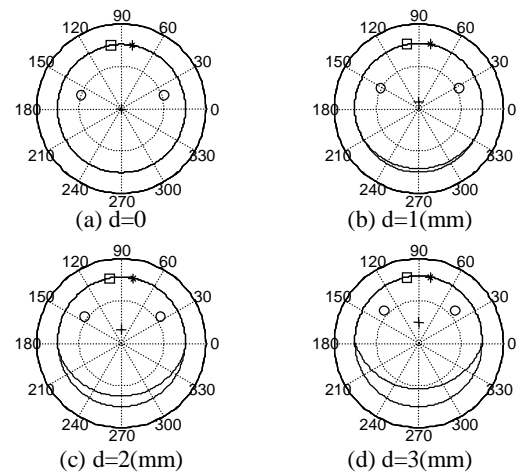


**Fig. 10 : Visualization of movement at case 2. It is shown that the reference point (denoted as '+') moves toward the middle point of two arteries as  $d$  increases.**

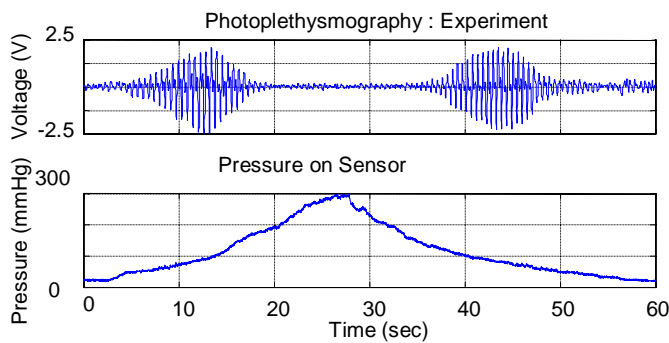


**Fig. 8 : Photoplethysmography and pressure at sensor unit from experiment in case 1**

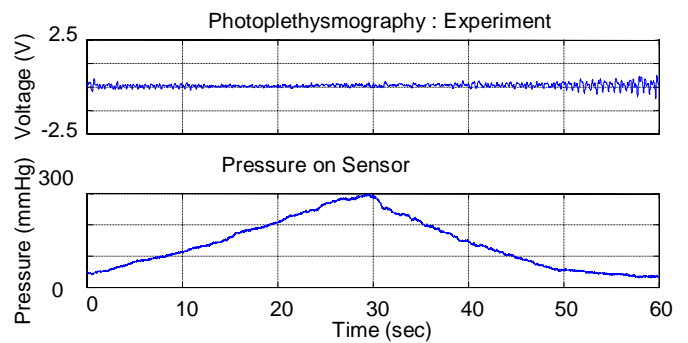


**Fig. 11 : Photoplethysmography and pressure at sensor unit from experiment in case 2**

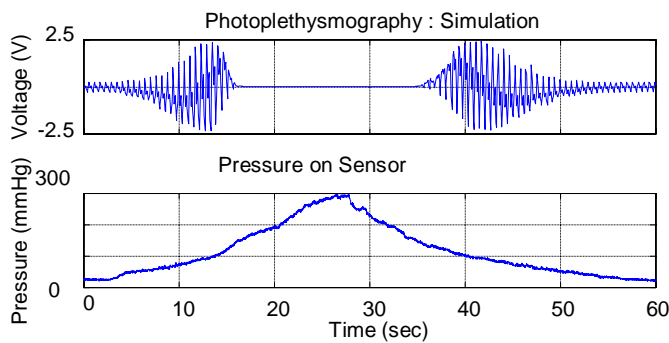


**Fig. 9 : Photoplethysmography and pressure at sensor unit from numerical simulation in case 1**

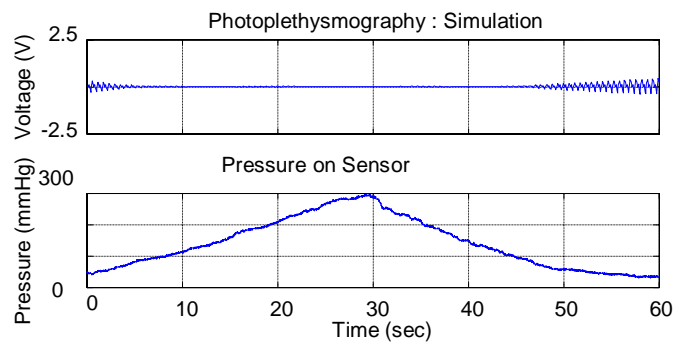


**Fig. 12 : Photoplethysmography and pressure at sensor unit from numerical simulation in case 2**

of digital artery. Secondly, as the direction of movement is aligned with the location of a digital artery, the external pressure around the artery which is  $P_o$  will increase quickly, resulting in the maximum pulsation point of the transmural pressure more easily. This will also give a more highly pulsating signal at the photodetector. Fig. 7 shows the numerical simulation of the finger and the ring configuration with a gradual increase of the displacement  $d$ . The large outer circle represents the ring, and the inner line which looks like a distorted circle is the finger surface. The two small circles inside the finger represent the two digital arteries, and the plus sign (+) inside the finger represents the reference point of the finger (which was denoted as point  $c$  in previous figures). It can be clearly seen that this reference point moves toward the direction of a digital artery as the displacement increases, and the digital artery goes closer to the LED and the photodetector which were represented as a small square (□) and a small star (\*) on the finger surface at around 20 degree respectively.

From the viewpoint of the arterial wall dynamics, it is expected that the amplitude of the photoplethysmograph will increase as the relative displacement of the finger to the ring increases up to a certain point where the transmural pressure goes to zero. After that peak point, the amplitude is expected to decrease since the digital artery will begin to be occluded. The simulation results and the experiment results are shown in Fig. 8 and Fig. 9 respectively. The upper plots of Fig. 8 and Fig. 9 are the photoplethysmographs, and the bottom figures are the pressures at the sensor unit. Both results show that there is a certain point of external pressure  $P_o$  that the amplitude of the photoplethysmograph becomes maximum. (The experiment result of case 1 shows a small oscillation even at very high external pressure. This is mainly due to the measurement noise and the signals at this region do not show the typical characteristics of human heart beats such as two peaks waveform.)

### **Analysis of the Simulation and Experiment : Case 2**

The second case is when the direction of finger movement is towards the middle point of the two digital arteries, i.e, to the palm side ( $\alpha=90^\circ$ ). In this case, the change of amplitude of the photoplethysmograph with finger displacement is not expected to be as great as in case 1 since the pressure increase at the artery is not as much as in case 1 with the same extent of displacement. In addition, as the distances of the two digital arteries from the sensor unit are geometrically longer than those of case 1, the overall amplitude of the photoplethysmography signal will not be large. This means that the amplitude of the photoplethysmograph will not change much even though the finger moves significantly to the direction of the palm side. Thus, it is expected that the amplitude of the signal will remain very small regardless of the finger displacement. (This is the worst configuration of the ring and the finger in terms of the signal to noise ratio as we observed in the experiments.) The movement of the finger in the ring is graphically visualized using our model in Fig. 10.

The experimental result is shown in Fig. 11, and the simulation result in Fig. 12. As was expected, the amplitude of the photoplethysmograph shows almost no change in experiment. In this configuration, it is even hard to recognize the pulse, in both experiment and simulation. In both results, the amplitude becomes a little larger with low pressures. This slight increase of the amplitude is from the pulsation of the capillaries on the palm side of the finger. Capillaries usually become occluded at an external pressure of around 10~35 mmHg since the internal blood pressure of the capillaries is around that range. This explains the disappearance of pulsation at higher pressures in the experiment result in case 2. (Small oscillation at high external pressures is mainly measurement noise.) In other

words, the photoplethysmograph of case 2 catches the pulsation from the capillaries when the external pressure is low. However, as the external pressure increases above 10~35 mmHg, this pulsation disappears as the capillaries become occluded. As the arterial pulsation cannot be apparently detected by the photoplethysmography at this configuration because the distance between the arteries and the sensor is long, we can see almost no pulsation with higher external pressures. Rather, the pulsation of the capillaries plays a major role with a low external pressure, although its amplitude is much smaller than that in case 1 in which the photoplethysmograph is mostly driven by arterial pulsation. The simulation result also exhibits a similar behavior

### **CONCLUSIONS**

A finger model for photoplethysmography of the Ring Sensor was developed. This model is an interdisciplinary physiological model that integrates an optical model, mechanical model, and the dynamics of the arteries and the capillaries. This model was verified by experiments and numerical simulations. This model is especially useful in describing the nature of the finger-based health monitoring device (the Ring Sensor). For example, from the viewpoint of noise minimization issues, there are many advantages of having this mathematical finger model in designing a ring sensor that is strong to noise caused by finger movement. As there are many design parameters that have to be tuned in the development of a ring sensor, this finger model will be a good analytic method in optimizing those parameters such as the compliance of the inner material of the ring and the configuration of the sensor. Further refinement of this model will focus on investigating the non-linearity of the finger tissue, as well as on more detailed modeling of the anatomical elements such as bones and skin layers.

### **REFERENCES**

- [1] Rhee, S., Yang, B-H. and Asada, H., "The Ring Sensor: a New Ambulatory Wearable Sensor for Twenty-Four Hour Patient Monitoring," Proc. of the 20<sup>th</sup> Annual International Conference of the IEEE Engineering in Medicine and Biology Society, Hong Kong, Oct, 1998
- [2] Yang, B-H., Rhee, S. and Asada, H., "A Twenty-Four Hour Tele-Nursing System Using a Ring Sensor," Proc. of 1998 IEEE International Conference on Robotics and Automation, Leuven, Belgium, May, 1998
- [3] Barker, S. J. and Shah, N. K., "The Effect of Motion on the Performance of Pulse Oximeters in Volunteers," *Anesthesiology*, 86, 101-108 (1997)
- [4] Plummer, J. L., Zakaria, A. Z., Ilsley, A. H., Fronsco, R. R. L. and Owen, H., "Evaluation of the Influence of Movement on Saturation Readings from Pulse Oximeters," *Anaesthesia*, 50, 423-426 (1995)
- [5] Vicente, L. M., Barreto, A. B. and Taberner, A., "Adaptive Pre-Processing of Photoplethysmographic Blood Volume Pulse Measurements," Southern Biomedical Engineering Conference - Proceedings Mar 29-31 1996 Sponsored by: University of Dayton; IEEE IEEE p 114-117
- [6] Higgins, J. L. and Fronek, A., "Photoplethysmographic Evaluation of the Relationship between Skin Reflectance and Skin Blood Volume," *Journal of Biomedical Engineering*, Vol 8, April, 130-136 (1986)
- [7] Wesseling, K. H., de Wit, B., van der Hoeven, G. M. A., van Groudoever, J. and Settels, J. J., "Physiocal, Calibrating Finger Vascular Physiology for Finapres,"

- Homeostatis, 36 (2-3), 67-82 (1995)
- [8] Feng, S., Zeng, F. and Chance, B., "Photon Migration in the Presence of a Single Defect : a Perturbation Analysis," *Applied Optics*, Vol. 34, No. 19, 3826-3837 (1995)
- [9] Tanaka, H. and Thulesius, O., "Effect of Temperature on Finger Artery Pressure Evaluated by Volume Clamp Technique," *Clinical Physiology* (1993) 13, 535-545
- [10] Yamakoshi, K., Shimazu, H., Shibata, M. and Kamiya, A., "New Oscillometric Method for Indirect Measurement of Systolic and Mean Arterial Pressure in the Human Finger. Part 1 : Correlation Study," *Medical & Biological Engineering & Computing* (1982), 20, 307-313